ORIGINAL PAPER

Tuning polymerization performance in ethylene–propylene copolymerization using a constrained geometry titanium catalyst [t-BuNSiMe$_2$(Me$_4$Cp)]TiMe$_2$: Insights from random and block copolymerization studies

Fengtao Li[1], Jing Wang[2], Xuelian He[1,*]

[1]*Shanghai Key Laboratory of Multiphase Material Chemical Engineering, East China University of Science and Technology, Shanghai 200237, China*

[2]*Sinopec Shanghai Petrochemical Co., Ltd*

*** Corresponding Author Email:** hexl@ecust.edu.cn

Received:18 April, Accepted: 29 May

DOI: 10.22063/POJ.2025.35685.1357

ABSTRACT

In this study, a titanium-based constrained geometry catalyst, [t-BuNSiMe$_2$(Me$_4$Cp)]TiMe$_2$, was synthesized and activated with methylaluminoxane for ethylene-propylene random and block copolymerization. The catalyst exhibited optimal activity at 70°C, yielding random copolymer chains with trace amounts of long polyethylene crystalline segments. When the ethylene content fell below 35%, random copolymers failed to crystallize. The block copolymerization system achieved maximum catalytic activity at a reaction temperature of 50°C and an ethylene block duration of 10 minutes. Shorter ethylene block durations correlated inversely with enhanced catalytic activity, increased molecular weight (peaking at 2.88×10^5 g/mol), and a narrower molecular weight distribution. The predominant component comprised extended PPP segments, constituting over 50% of the total copolymer composition. Within the polymer chains, propylene monomers were primarily incorporated as PPP and PPE structural motifs. Moreover, a progressive decrease in [PPP] content was observed with increasing ethylene block duration, whereas [PPE] content exhibited the opposite trend. This inverse relationship suggested that PPP segments gradually transform into PPE configurations via ethylene monomer insertion. These findings demonstrated that product structure and properties can be effectively tuned by adjusting initial monomer feed ratios or the timing of monomer block introduction.

Keywords: Constrained geometry titanium-based catalyst; titanium-based catalyst; ethylene-propylene copolymerization; ethylene–propylene copolymers; block copolymerization.

INTRODUCTION

Ethylene-propylene copolymers (EPM/EPDM), an important subclass of polyolefin elastomers, are widely used in automotive seals, construction waterproofing, wire and cable insulation, films, and polymer modification due to their excellent low-temperature resistance, aging stability, and flexibility [1]. Among the major synthetic rubber types, ethylene-propylene rubber (EPR) has shown the most rapid development in recent decades [2].

Although traditional Ziegler-Natta catalysts are commonly used for ethylene-propylene copolymerization,

their multi-active-site characteristic leads to uneven monomer distribution and broad molecular weight disperse on (MWD), limiting precise control over copolymer structure and performance [3]. Currently, homogeneous vanadium catalysts are widely used in industry to produce fully amorphous EPR, but they still face inherent limitations in both product performance and process efficiency. Recent advances in metallocene catalysts, owing to their single-site characteristics, have enabled sequence-controlled synthesis of EPR copolymers [4]. Notably, the pioneering $Cp_2Zr(CH_3)_3$/MAO catalytic system reported by Kaminsky and Miri [5] demonstrates significantly enhanced activity (2100 kg/(molZr·h·bar)) compared with vanadium-based catalysts (860 kg/(molV·h·bar)) [6].

Furthermore, these systems exhibit low propylene insertion rates, with ethylene content reaching 71 wt%. Consequently, optimizing ligand structures in metallocene catalysts to enhance monomer insertion efficiency and distribution has become a key research focus for developing high-performance copolymers.

Catalyst architecture profoundly impacts catalytic activity and copolymer properties. Asymmetric bridged catalysts demonstrate superior performance in ethylene-propylene copolymerization. Chien and He[7] compared various metallocene catalysts, including non-bridged (Cp_2ZrCl_2, Cp_2TiCl_2, Cp_2HfCl_2) and bridged types ($Et(Ind)_2ZrCl_2$, $Et(IndH_4)_2ZrCl_2$), revealing that the bridged $Et(Ind)_2ZrCl_2$ achieved exceptional activity (10^4 kg/(molZr·h·bar)) with enhanced propylene insertion. Similarly, Uozumi and Soga[8] investigated non-bridged, bridged-symmetric, and bridged-asymmetric catalysts (CpZrCly/MAO, $Et(IndH_4)$ZrCly/MAO, i-Pr(Cp)(Flu)ZrCly/MAO) under ambient pressure (40°C), demonstrating through ^{13}C NMR analysis that asymmetric bridged catalysts significantly favor propylene insertion.

Building on these findings, Dow Chemical patented a series of constrained geometry catalysts (CGCs). These asymmetric bridged catalysts impose geometric constraints on the metal center, thereby improving propylene copolymerization efficiency and thermal stability at elevated temperatures. This breakthrough established CGCs as ideal systems for high-performance EPR production, accelerating industrial applications and premium product development [9].

Wu et al. [10] systematically investigated the rheological properties of CGC-synthesized polyolefin elastomers (EPDM Nordel IP and POE Engage) using $[t\text{-}BuNSiMe_2(Me_4Cp)]TiCl_2$ with INSITETM technology. Compared with conventional EPDM and POE, these materials exhibit superior purity, structural control, and uniformity: Walton et al. [11] developed CGC-derived EPR with >90 wt% ethylene content, achieving a 25% improvement in wear resistance for natural rubber composites while maintaining sulfur vulcanization compatibility. This enabled the development of polyethylene-like foam materials compatible with sulfur curing.

Wang et al. [12] developed a catalyst design methodology that integrates density functional theory (DFT) with artificial neural networks (ANN). Through optimization of the ANN model (R2 = 0.99704), they successfully predicted and designed a series of novel CGC catalysts, achieving catalytic activities ranging from 145 - 150 kg product/g M. Comparative analysis demonstrated that β-site substitution of the cyclopentadienyl group is crucial to the catalytic activity of CGC catalysts, while conjugated cyclic groups (e.g., phenyl, pyridyl) significantly enhance activity.

This study introduces a constrained geometry configuration (CGC) titanium catalyst, [t-BuNSiMe$_2$(Me$_4$Cp)]TiMe$_2$, and applies it in ethylene-propylene block copolymerization. The catalyst's unique spatial structure enhances propylene insertion rates, while the pre-methylation of the central metal atom reduces co-catalyst requirements, thereby lowering associated costs.

EXPERIMENTAL

Materials

Reagents sensitive to moisture and oxygen were handled using standard Schlenk techniques, either under high-purity nitrogen or in a glove box filled with nitrogen. Prior to use, high-purity nitrogen was passed through a 4Å molecular sieve column for dehydration and an Ag column for deoxygenation before being introduced into Schlenk bottles. All glassware and reagent transfer needles were dried in an oven at 120℃ for over 3 hours to remove moisture and then cooled under nitrogen protection before use.

Solvents such as n-hexane, tetrahydrofuran (THF), and ether were purified by removing moisture and oxygen prior to use. N-hexane was refluxed for several hours in a distillation setup. After cooling, the distillate was transferred to a glove box for storage. THF and ether were treated with calcium hydride and stirred for several hours to remove moisture. High-purity nitrogen was bubbled through the solvents for several hours to remove oxygen before transferring them to a glove box.

Synthesis of [t-BuNSiMe$_2$(Me$_4$Cp)]TiMe$_2$ complex

Synthesis of 2,3,4,5-Me$_4$Cp

1.88 g LiAlH$_4$ was added to 50 mL diethyl ether in a 200 mL Schlenk flask. While stirring, 6 mL 2,3,4,5-tetramethyl-2-cyclopentenone was added. The mixture was cooled to 0 °C for 30 minutes and then stirred overnight at room temperature. After quenching with water, the organic phase was extracted, dried, and concentrated under reduced pressure to afford 2,3,4,5-tetramethylcyclopentadiene (75%) [13].

Synthesis of (Me$_4$Cp)Li

30 mmol of 2,3,4,5-Me$_4$Cp was dissolved in 50 mL THF in a Schlenk flask inside an argon-filled glove box. After cooling to -78 °C, 14.4 mL of n-butyllithium (2.5 mol/L) was added dropwise. The mixture was stirred overnight, yielding a yellowish (Me$_4$Cp)Li solution.

Synthesis of (Me$_4$Cp)Me$_2$SiCl$_2$

8.3 mL of Me$_2$SiCl$_2$ and 35 mL of THF were mixed and cooled to -78 °C. The (Me$_4$Cp)Li solution was added slowly, forming a pale yellow solution. The reaction proceeded for 3 h at low temperature, then overnight at room temperature. The solvent was removed under reduced pressure, yielding a pale yellow oil (83%).

Synthesis of $Me_4CpMe_2Si(t\text{-}BuNH)$

20 mmol $(Me_4Cp)Me_2SiCl_2$ and 50 mL n-hexane were mixed in a Schlenk flask. After cooling to 0 °C, 2.48 g tert-butylamine was added. The reaction was stirred at low temperature for 30 min and then overnight at room temperature. The solvent was removed, and the product was purified with n-hexane, yielding a yellow oil (92%) (Scheme 1).

Synthesis of $[t\text{-}BuNSiMe_2(Me_4Cp)]TiMe_2$ complex

1.26 g $(Me_4Cp)Me_2Si(t\text{-}BuNH)$ was dissolved in 50 mL THF in a glove box. At -78°C, 10 mL MeLi (1.6 mol/L) was added dropwise. The solution was stirred overnight, forming a ligand dilithium salt solution. The solution was then added to 0.45 mL TiCl4 in n-hexane and stirred for several hours. After filtration and washing with n-hexane, 2.67 mL of MeBrMg (3.0 mol/L) was added. The final product crystallized at low temperatures, yielding olive-green crystals (40%) (Scheme 2).

Copolymerization of ethylene and propylene

A semi-continuous solution polymerization process is used to catalyze propylene polymerization, with the entire setup placed in a nitrogen-filled glove box to avoid water and oxygen interference. The reaction is conducted in a 300 mL Parr stainless steel reactor, equipped with a heating jacket and control console. After preheating at 120°C for 1 hour, the reactor is quickly transferred to the glove box and allowed to cool to room temperature. Cyclohexane and MAO are added as co-catalysts, and the catalyst solution is stored in a separate stainless steel catalyst reservoir. High-purity nitrogen (0.3-0.5 MPa) is introduced to ensure the catalyst is fully transferred into the reactor. The reactor is stirred and heated to the desired temperature, and ethylene and propylene gases are introduced at the specified pressures. Once gas dissolution is balanced, the catalyst is added to start the polymerization. After the reaction, the propylene inlet valve is closed, and nitrogen is used to purge the reactor. The reaction mixture is then discharged, quenched in an HCl/ethanol solution, washed with ethanol, dried, and weighed to calculate activity.

For random copolymerization, ethylene and propylene were premixed at specified partial pressure ratios (3/7, 4/6, 5/5, 6/4, 7/3) in a stainless steel high-pressure gas-mixing vessel, serving as the monomer feed for ethylene-propylene copolymerization. In block copolymerization, propylene was introduced exclusively at the initial stage. After 10 minutes, the reactor was depressurized to remove residual propylene, followed by a rapid switch to ethylene feed, allowing polymerization to proceed for a predetermined duration before termination.

Characterization

The compounds' NMR spectra (^1H and ^{13}C) were recorded on a Bruker Ascend 600M spectrometer using deuterated chloroform ($CDCl_3$) as the solvent and tetramethylsilane (TMS) as the internal standard. Prior to use, $CDCl_3$ was deoxygenated and desiccated by purging with high-purity nitrogen and soaking in 4Å molecular sieves for 48 hours in a glove box. The sample preparation involved weighing approximately 10 mg of the sample in an NMR tube, adding a small amount of CDCl3, and sealing the tube for rapid analysis. The

chemical shifts of the solvent peaks were 7.26 ppm and 77.06 ppm for ^{1}H and ^{13}C NMR, respectively.

The differential scanning calorimetry (DSC) measurements of the complexes and polymer products were carried out using a TA Q2000 system. Approximately 5 mg of the sample was sealed in an aluminum pan and heated under a nitrogen atmosphere at a rate of 10°C/min, from room temperature to 250°C. The polymer products were heated to 160°C at 10 °C/min, held for 5 minutes to eliminate thermal history, then cooled to -20°C, and heated back to 160°C. T_g was calculated from the heat flow curve during the second heating cycle.

Single crystals of the complex were obtained by crystallizing from hexane for 24 hours, yielding yellow-green crystals. Crystals were mounted on clean glass slides with crystal glue, and selected under a microscope. X-ray diffraction data were collected at 173 K using a Bruker APEX2 diffractometer with MoK α radiation (λ = 0.71073 Å). The crystal structure was solved using direct methods and refined by least squares.

The molecular weight and distribution of the polymers were measured using high-temperature gel permeation chromatography (HT-GPC, PL220, PolyLab Co.). Samples were dissolved in 1,2,4-trichlorobenzene (TCB) at 160 °C and filtered before analysis. The test conditions included a flow rate of 1.0 mL/min, using TCB as the mobile phase, and PS as the standard. M_w and M_n were determined from the GPC data.

The composition and sequence structure of ethylene-propylene copolymers were determined using a Bruker Inova 500M NMR spectrometer. Samples were dissolved in deuterated 1,2-dichlorobenzene (concentration ~10 wt%) with 5 mg of chromium acetylacetonate as a relaxation agent, and heated at 120 °C for 4-6 hours. The test conditions included a frequency of 126 MHz, a sample time of 0.6 s, a pulse delay of 3 s, and 200 scans at 140 °C.

The catalyst activity is calculated as follows: $Activity = \frac{m}{1000n \cdot t}$

where m is the polymer mass (g), n is the molar number of the main catalyst (mol), and t is the polymerization time (h).

RESULTS AND DISCUSSION

Structure of [t-BuNSiMe$_2$(Me$_4$Cp)]TiMe$_2$ complex

As shown in Figure 3.1, the complex was characterized by ^{1}H NMR ($CDCl_3$): δ 2.15 (s, 6H, Cp-CH_3), 1.90 (s, 6H, Cp-CH_3), 1.55 (s, 9H, NC(CH_3)$_3$), 0.46 (s, 6H, Si-CH_3), and 0.16 (s, 6H, Ti-CH_3). The spectrum confirms that titanium successfully coordinated with the ligand, and the two chlorine atoms on the Ti center were replaced by methyl groups (CH_3), resulting in the formation of a Si-N-Ti-Cp quaternary ring structure complex with Cs mirror symmetry in solution.

Figure 3.2 shows the carbon nuclear magnetic resonance (^{13}C NMR) spectrum of [t-BuNSiMe$_2$(Me$_4$Cp)]TiMe$_2$. The spectrum reveals the following chemical shifts: δ 133.34, 129.48, 97.39, 57.63, 50.13, 34.35, 14.36, 11.89, and 5.94 ppm. The peak at 77.06 ppm is attributed to the solvent. The three

peaks between 5 - 15 ppm correspond to the five carbons (C1-C5) on the cyclopentadienyl ring, while the two peaks between 125-135 ppm correspond to the four methyl carbons (C6-C9) on the cyclopentadienyl ring, indicating the symmetry of the cyclopentadienyl ring structure. Distinct peaks observed for the methyl carbons of the titanium methyl, silicon methyl, and amine groups suggest that these methyl groups share the same chemical environment and are equivalent in molecular structure. This finding is consistent with the hydrogen NMR data, further supporting the presence of a symmetry plane in the molecular structure of the complex in solution, with the overall structure exhibiting Cs symmetry.

The molecular structure of the complex was determined using single-crystal X-ray diffraction, and the crystal cell stacking diagram is presented in Figure 3.3. According to the XRD data, the [t-$BuNSiMe_2(Me_4Cp)]TiMe_2$ complex possesses a symmetry plane in the solid state and exhibits an overall Cs symmetry. The bond lengths between the central titanium atom and the five carbon atoms (C1-C5) of the cyclopentadienyl ligand range from 2.284 to 2.461 Å. In this complex, the cyclopentadienyl ligand coordinates with the titanium atom in an η5 fashion, consistent with previous reports [14]. Additionally, compared with the nuclear magnetic resonance (NMR) spectrum, the complex also shows Cs symmetry in solution.

Copolymerization of ethylene and propylene

The effect of temperature on ethylene-propylene random copolymerization

The effect of varying temperatures on ethylene-propylene random copolymerization results is summarized in Table 1.

According to Table 1, within the temperature range of 40 - 70 ℃, the copolymerization activity increases progressively with an increase in polymerization temperature[25]. A marked enhancement in copolymerization activity occurs when the temperature rises from 50 °C to 60 °C. At a reaction temperature of 70 °C, the copolymerization activity reaches its peak value of 3.28×10^3 $kg\cdot mol^{-1}\cdot h^{-1}$. Compared to conventional systems, this catalyst shows superior stability at elevated temperatures[26].

As the reaction temperature increases, the glass transition temperature (*T*g) of the polymer decreases slightly; however, the variation remains insignificant. The melting temperature (*T*m) of the copolymer is close to but slightly lower than that of polyethylene, indicating the presence of a limited number of relatively long ethylene chain segments within the copolymer, which is characteristic of polymers commonly obtained via polymerization catalyzed by CGCs[15]. Additionally, the incorporation of propylene disrupts the crystalline structure of polyethylene, leading to reduced crystallinity, as further confirmed by the observed crystallization temperature (*T*c). Notably, when the polymerization temperature reaches 70 °C, no distinct crystallization temperature is detected, suggesting a uniform monomer distribution within the copolymer, shorter polyethylene segments, and incomplete crystallization.

Effect of ethylene/propylene feed pressure ratio on ethylene-propylene random copolymerization

The impact of varying ethylene/propylene feed pressure ratio (E/P) on the ethylene-propylene

copolymerization results is presented in Table 2.

The polymerization activity initially decreases and then increases with the rising propylene content in the comonomer. When the E/P is 5/5, the copolymerization activity reaches its lowest value of 2.38×10^3 kg·mol^{-1}·h^{-1}. This trend arises from the competitive diffusion and insertion of ethylene and propylene monomers into active sites during copolymerization. When the E/P is 1/1, this competition is at its peak, leading to mutual interference and a subsequent decline in copolymerization activity. The deviation observed for Entry 4 is attributed to the relatively high ethylene content in the comonomer, while the catalytic system exhibits slightly lower selectivity for ethylene than for propylene, thereby reducing polymerization activity. In Entry 8, where the propylene content in the comonomer is the highest, the copolymerization activity reaches a maximum of 5.15×10^3 kg·mol^{-1}·h^{-1}. Meanwhile, when the E/P is 5/5, the propylene content in the polymer reaches 55 mol%, surpassing that typically achieved with conventional catalysts such as *rac*-Et(Ind)$_2$ZrCl$_2$. This demonstrates an enhanced propensity for propylene incorporation by the catalyst under investigation[16].

In order to better analyze the monomer content and segment sequence distribution in ethylene propylene copolymers, we used high-temperature 13C NMR as a characterization method and processed the obtained results. In order to determine the monomer content in ethylene propylene copolymers, Carman et al. [17] classified the carbon atoms in the copolymers into three categories: methyl carbon, methylene carbon, and methylene carbon, named P, S, and T respectively. To indicate the difference in chain structure near the target atom, a notation using two Greek letters as subscripts has been adopted to indicate the distance between the target carbon atom and the nearest tertiary carbon at either end of the copolymer molecular chain[20]. Randall et al.[18] summarized the chemical shift assignments for different sequence units in ethylene-propylene copolymers. Based on the computational approach proposed by Kakugo[19], the distributions of binary and ternary sequences were determined from 13C NMR data, revealing the impact of the ethylene/propylene monomer ratio on the composition and sequence distribution of ethylene-propylene random copolymers. The results are shown in Figure 3.4 and Table 3.

Comparative analysis indicates that the propylene content in the copolymer is slightly higher than in the monomer mixture, further confirming the catalytic system's slightly greater selectivity for propylene over ethylene. Within the E/P range of 7/3 to 4/6, the copolymerization parameter product rE·rP<1 suggests that the resulting ethylene-propylene copolymer is random [18]. As the propylene content in the monomer feed increases, the concentrations of [P], [PP], and [PPP] gradually rise, while those of [E], [EE], and [EEE] decline. In ternary copolymer sequences, the contents of [PPE] and [PEP] generally increase with higher propylene feed content, whereas [EEP] and [EPE] decrease.

Notably, when the E/P is 3/7, the [PPP] content increases significantly, while [EEE] also exhibits a slight rise. This trend suggests a tendency for the reaction system to form block copolymers, reducing the proportion of random EP sequences and consequently increasing the relative contents of PP and EE sequences, which is further validated by rE·rP>1. Additionally, the peak at a chemical shift of 33.1 ppm corresponds to crystalline polyethylene segments, and its intensity decreases as the ethylene content in the monomer feed declines, indicating a reduction in the length of polyethylene segments within the copolymer.

Meanwhile, as the propylene content in the monomer feed increases, the random index (RI) of the copolymer decreases progressively from 0.75 (E/P = 7/3) to 0.43 (E/P = 3/7). This index characterizes the homogeneity of comonomer distribution along the copolymer chain, representing the percentage of monomer units not incorporated into homopolymer segments consisting of three or more identical monomer units. A decrease in RI signifies an increased proportion of units embedded within long homopolymer segments, a rise in the heterogeneity of copolymer distribution, and a shift in comonomer arrangement along the molecular chain from random/alternating toward a block-like distribution.

As shown in Table 2, the glass transition temperature (T_g) of the ethylene-propylene copolymers falls between that of polyethylene (<-60 °C) and polypropylene (approximately 0°C). Even slight variations in monomer composition significantly influence the copolymers' thermal properties. As the ethylene content in the monomer feed decreases, the T_g of the copolymer increases noticeably. Specifically, when the E/P decreases from 7/3 to 3/7, the T_g rises from -50.08 °C to -25.01 °C.

Furthermore, both *T*m and *T*c of the copolymers gradually decrease with the reduction of ethylene content. This trend arises because a lower ethylene fraction in the copolymer disrupts the formation of long ethylene segments, thereby shortening the crystallizable ethylene sequences. When the ethylene content falls below 35%, the ethylene sequences become too short to crystallize.

Figure 3.5 illustrates the effect of the E/P on the molecular weight and its distribution in ethylene-propylene copolymers. A comparative analysis reveals that, under the same catalytic system, the introduction of ethylene monomers results in a significantly lower molecular weight for ethylene-propylene copolymers compared with polypropylene homopolymers. As shown in Figure 3.5 and Table 2, the molecular weight and its distribution exhibit minimal variation with changes in the E/P. The number-average molecular weight (M_n) remains stable in the range of 1.74 - 2.33×10^4 g/mol, while the polydispersity index (PDI) stays between 2.42 to 2.84. When the E/P is 1:1, competition between ethylene and propylene monomers for diffusion and insertion into active centers reduces polymerization activity, leading to a decrease in the molecular weight of the resulting copolymer. For E/P < 1, as the propylene content in the monomer feed increases, the molecular weight of the product exhibits a slight increase, and the PDI narrows slightly, unlike observations in conventional metallocene systems[22]. This phenomenon can be attributed to the preferential insertion of propylene monomers into the growing polymer chain.. The CGC catalyst system demonstrates a greater propensity for propylene monomer incorporation compared to conventional metallocene systems[23,24].

Effect of temperature on the P-E block copolymerization

The effect of different temperatures on the propylene-ethylene block copolymerization results is shown in Table 4.

As shown in Table 4, the block copolymerization activity initially increases and then decreases as the polymerization temperature rises within the range of 30 – 70 °C. The highest block copolymerization activity of 8.15 ×10^3 kg·mol^{-1}·h^{-1} is achieved at 50°C, more than twice the activity at 30 °C. As the temperature

continues to rise, the polymerization activity gradually decreases. This behavior is attributed to the slower polymerization rate at lower temperatures, which results in lower catalytic activity. However, once the temperature exceeds the optimal value, the polymerization activity begins to decline due to an increasing degree of catalyst deactivation.

In comparison with the random copolymer, the block copolymer has a significantly higher T_g, indicating the polymerization method (propylene polymerized first, followed by ethylene) results in a copolymer with fewer ethylene segments and lower ethylene content.

Analysis of Table 4 reveals that as the polymerization temperature increases, T_g of the block copolymer gradually decreases. When the polymerization temperature reaches 70 °C, the T_g reaches its lowest value of -19.39 °C, indicating that higher polymerization temperatures promote greater incorporation of ethylene monomers into the copolymer. A comparative analysis indicates that T_g of the block copolymer is significantly higher than that of the random copolymer, suggesting that a polymerization sequence initiated with propylene polymerization followed by ethylene incorporation leads to a block copolymer with lower ethylene content and shorter ethylene segment lengths.

Effect of ethylene insertion time on P-E block copolymerization

The data presented in Section 3.2.3 revealed that the copolymer produced through the polymerization method, where propylene was polymerized for 10 minutes followed by ethylene polymerization for an additional 10 minutes, resulted in a copolymer with a low ethylene content. To enhance the ethylene content in the polymer, this study extends the ethylene insertion time $t_{(E)}$ to 20, 25, 30, and 40 minutes. The impact of variations in the ethylene insertion time on the composition and properties of the block copolymer is subsequently analyzed.

The results of the effect of the ethylene insertion time on the P-E block copolymerization are presented in Table 5.

As shown, with the increase in $t_{(E)}$, the copolymer yield increases only slightly, resulting in a decrease in polymerization activity per unit time. When $t_{(E)}$ reaches 40 minutes, the copolymerization activity decreases to its lowest point of 3.92 $\times 10^3$ kg·mol^{-1}·h^{-1}, which is approximately half of the activity observed in Entry 11. This reduction is attributed to the catalytic system's higher polymerization activity for propylene compared with ethylene. Furthermore, as the reaction time increases, the degree of catalyst deactivation also rises, and with the extension of $t_{(E)}$, the number of active sites in the reaction system gradually diminishes, ultimately leading to a decrease in polymerization activity.

The effect of $t_{(E)}$ on the composition and sequence distribution of P-E block copolymers is illustrated in Figure 3.6 and Table 6. The results indicate that as $t_{(E)}$ is extended, the ethylene content in the copolymer gradually increases. When $t_{(E)}$ is 10 minutes, the ethylene content is only 9 mol%, and no [EEE] segments are present. However, when $t_{(E)}$ reaches 40 minutes, the ethylene content increases to a maximum of 23 mol%, accompanied by an increase in the [EEE] segment content. Furthermore, when $t_{(E)}$ is extended to 25 minutes, a characteristic peak at 33.1 ppm, corresponding to crystalline polyethylene segments, emerges, although its intensity remains relatively small. Further extension of $t_{(E)}$ leads to only a slight increase in the peak intensity,

indicating that while the ethylene segments grow, the change is minimal. A comparative analysis reveals that the [EEE] content in the block copolymer is much lower than in the random copolymer, suggesting that the block copolymer contains very few long ethylene segments, with the ethylene monomers primarily existing in the forms of PPE and EEP. The experimental data indicate that the dominant component of the block copolymer is the long PPP segment, which accounts for more than half of the total copolymer. The propylene monomer is primarily present in the form of PPP and PPE within the polymer chain. As $t_{(E)}$ increases, the content of [PPP] gradually decreases, while the content of [PPE] increases, suggesting that as ethylene monomers are incorporated, some PPP segments are gradually converted into PPE. Finally, the copolymerization rate product $rE \cdot rP > 1$ confirms that the resulting copolymer is of the block type. Simultaneously, as the $t_{(E)}$ increases, the random index (RI) of the copolymer rises progressively from 0.101 ($t_{(E)}$ = 10 min) to 0.492 ($t_{(E)}$ = 40 min). This increase in RI signifies a reduction in long monomer sequences, a concomitant rise in the proportion of short sequences, and a more uniform and random distribution of ethylene and propylene units along the polymer chain [21]. Consequently, the comonomer arrangement shifts from a block-like distribution toward a random/alternating configuration along the molecular chain.

According to Table 5, as $t_{(E)}$ increases, T_g of the block copolymer gradually decreases. This decrease is attributed to the increasing ethylene content in the copolymer, which enhances the flexibility of the polymer chains. In contrast to the ethylene-propylene random copolymer, the block copolymer does not exhibit distinct *T*c and *T*m values. A small melting peak is observed only when $t_{(E)}$ reaches 40 minutes, but no crystallization is detected. This suggests that although the ethylene segments gradually grow with the extension of $t_{(E)}$, their length remains insufficient for crystallization.

Figure 3.7 illustrates the variation in the molecular weight and molecular weight distribution of P-E block copolymers as a function of $t_{(E)}$. As shown in the data from Table 5, it is observed that as $t_{(E)}$ increases, the molecular weight of the copolymer gradually decreases, accompanied by a widening of the PDI. This phenomenon can be attributed to the extension of the reaction time, during which ethylene monomers insert into the growing propylene chains. Concurrently, a small fraction of new chains is initiated, resulting in a broader molecular weight distribution. In comparison, the molecular weight of the block copolymers is notably higher than that of the random copolymers, which can be ascribed to the absence of competition between ethylene and propylene during the early stages of polymerization. The variation pattern of molecular weight is similar to that in previous literature, and the block copolymer obtained by this catalyst has a higher molecular weight [27].

CONCLUSION

This study synthesizes a constrained-geometry titanium catalyst, [t- $BuNSiMe_2(Me_4Cp)]TiMe_2$, via a diprotonic method and investigates its application in ethylene- propylene copolymerization using the [t- $BuNSiMe_2(Me_4Cp)]TiMe_2$/MAO catalytic system. The catalyst's asymmetric geometry enhances propylene insertion efficiency, while pre- methylation at the titanium center reduces co-catalyst requirements, offering cost advantages. Two feeding strategies are employed to synthesize random and block copolymers. In random

copolymerization, the effects of temperature and monomer molar ratio are examined, revealing optimal catalytic activity (3.28×10^3 kg·mol^{-1}·h^{-}1) at 70 °C. The resulting polymers contain minimal long crystalline polyethylene segments, with crystallization eliminated when propylene content exceeds 35%. In block copolymerization, the maximum polymerization activity (8.15×10^3 kg·mol^{-1}·h^{-1}) is achieved under copolymerization conditions at a reaction temperature of 50°C with a $t_{(E)}$ of 10 minutes. Propylene predominantly incorporates PPP and PPE sequences, with PPP segments constituting more than 50% of polymer chains. Shorter ethylene block durations enhance catalytic activity, increase molecular weight (maximum 2.88×10^5 g/mol), and narrow the polydispersity (minimum PDI 2.35). Key findings demonstrate that feeding protocols significantly influence copolymer composition and molecular characteristics. Composition modulation can be achieved through adjustments in initial monomer ratios or block duration. The results establish structure-property correlations essential for tailoring copolymer performance.

ACKNOWLEDGEMENT

This work was financially supported by the National Natural Science Foundation of China (Grant No. 22278141).

REFERENCES

1. Fan GQ (2017) Ethylene/propylene copolymerization by metallocene catalyst: Mechanisms of initiation, propagation and termination. Petrochemical Technology 46(6): 708-714
2. Galland PG, Vuluga G (2004) Polyolefins: The most promising large-volume materials for the 21st century. J Polym Sci Pol Chem 42: 396-415 [CrossRef]
3. Chum PS, Swogger KW (2008) Olefin polymer technologies—History and recent progress at The Dow Chemical Company. Prog Polym Sci 33: 797-819 [CrossRef]
4. Zhang X F, Wang W, Zhang LG, Zhuo J, Zheng G, Qiao JL, Mao BQ (2021) Progress in the single-site catalysts and the corresponding polyolefin materials. Polym Mater Sci Eng 37: 141-149
5. Kaminsky W, Miri M (1985) Ethylene propylene diene terpolymers produced with a homogeneous and highly active zirconium catalyst. J Polym Sci, Polym Chem 23: 2151-2164 [CrossRef]
6. Hu J, Zhu BC, Yi JJ, Wang JM (2010) Metal organic olefin polymerization catalysts and their polyolefins. Beijing, Chemical Industry Press (in Chinese)
7. Chien JCW, He D (1991) Olefin copolymerization with metallocene catalysts. I. Comparison of catalysts. J Polym Sci Pol Chem 29: 1585-1593 [CrossRef]
8. Uozumi T, Soga K (1992) Copolymerization of olefins with Kaminsky-Sinn-type catalysts. Makromol Chem 193(4): 823-831 [CrossRef]

9. Stevens J C, Neithamer D R (1992) Metal complex compounds, process for preparation and method of use: EP0418044 A2

10. Wu Q, Li P, Mu J, Zhang N, An P, Wu, J (2006) The rheological behavior of EPDM Nordel IP and POE Engage produced by CGC and INSITE™ technology. J Appl Polym Sci 101: 2847-2853 [CrossRef]

11. Walton KL, Hughes MM, Parikh DR (2001) A new class of ethylene-propylene-diene terpolymers produced from constrained geometry metallocene catalysts. Rubber Chem Technol 74: 689-700 [CrossRef]

12. Wang S, Zhuo X, Fan H, Cao C, Jiang T, Yan B (2024) Computer-assisted design of CGC catalysts for ethylene/1-octene copolymerization: A combined DFT and artificial neural network approach. Polymer 300: 126997 [CrossRef]

13. Fendrick CM, Schertz LD, Day VW, Marks TJ (1988) Manipulation of organoactinide coordinative unsaturation. Synthesis, structures, and reactivity of thorium hydrocarbyls and hydrides with chelating bis(tetramethylcyclopentadienyl) ancillary ligands. Organometallics 7: 1828-1838 [CrossRef]

14. Ammendola P, Vitagliano A, Oliva L (1984) Ethylene-propene copolymerization in the presence of a ^{13}C enriched catalyst: End group analysis and monomer reactivities in the first insertion steps. Makromol Chem, 185: 2421-2428 [CrossRef]

15. Dashti A, Ahmadi M, Haddadi-Asl V, Ahmadjo S, Mortazavi S (2023) Tandem coordinative chain transfer polymerization for long chain branched Polyethylene: The role of chain displacement. Eur Polym J 190: 112008 [CrossRef]

16. Dashti A, Ahmadi M, Haddadi-Asl V. (2023) Kinetics controlled microstructure and composition in coordinative chain transfer copolymerization of ethylene–propylene. J Mol Liq 385: 122284 [CrossRef]

17. Wilkes CE, Carman CJ, Harrington RA (1973) Monomer sequence distribution in ethylene-propylene terpolymers measured by ^{13}C nuclear magnetic resonance. J Polym Sci Polym Symp 43(1): 237-250 [CrossRef]

18. Randall JC, Hsieh E T (1982) Carbon-13 NMR tetrad assignments in ethylene-propylene copolymers. Macromolecules 15(6): 1584-1586 [CrossRef]

19. Kakugo M, Naito Y, Mizunuma K, Miyatake T (1982) Carbon-13 NMR determination of monomer sequence distribution in ethylene-propylene copolymers prepared with δ-titanium trichloride-diethylaluminum chloride. Macromolecules 15: 1150-1152 [CrossRef]

20. Carman CJ, Harrington RA, Wilkes CE (1977) Monomer Sequence Distribution in Ethylene-Propylene Rubber Measured by ^{13}C NMR. Rubber Chemistry & Technology 10: 149-167 [CrossRef]

21. Omidvar M, Ahmadjo S, Mortazavi MM, Beheshti M (2025) Deciphering the function of $Zn(Et)_2$ in tailoring comonomer insertion sequence during coordinative chain transfer ethylene/propylene copolymerization. Appl Catal-A 691: 120069 [CrossRef]

22. Guo Y, Zhang Z, Guo W, Khan A, Fu z, Xu J, Fan Z (2017) Kinetics and mechanism of metallocene-catalyzed olefin polymerization: Comparison of ethylene, propylene homopolymerizations, and their copolymerization. J Polym Sci Pol Chem 55: 867-875 [CrossRef]

23. Faingol'd EE, Saratovskikh SL, Panin AN, Babkina ON, Zharkov IV, Garifullin NO, Shilov GV, Bravaya NM (2021) Ethylene/propylene and ethylene/propylene/5-ethylidene-2-norbornene copolymerizations on metallocene/(2,6-tBu_2PhO-)AliBu_2 catalyst systems. Polymer 220: 123559 [CrossRef]

24. Park S, Wang WJ, Zhu SP (2000) Continuous solution copolymerization of ethylene with propylene using a constrained geometry catalyst system. Macromol Chem Phys 201(16): 2203-2209 [CrossRef]

25. Mansouri S, Omidvar M, Mortazavi SM, Ahmadjo S (2022) 5-Ethylidene-2-norbornene polymerization by α-diimine nickel catalyst: A revealing insight into the pivotal function of binuclear and mononuclear catalyst structure in tailoring polymer architecture. Macromol React Eng 16: 2100052 [CrossRef]

26. Omidvar M, Mansouri S, Mortazavi SM, Ahmadjo (2024) Shedding light on the poly (5-ethylidene-2-norbornene) microstructural differences: Skeleton rearrangements during polymerization. Journal of Applied Polymer Science, 141(2): e54775 [CrossRef]

27. Eagan JM, Xu J, Di Girolamo R, Thurber CM (2017) Combining polyethylene and polypropylene: Enhanced performance with PE/iPP multiblock polymers. Science, 355: 814-816 [CrossRef]

Figure Captions

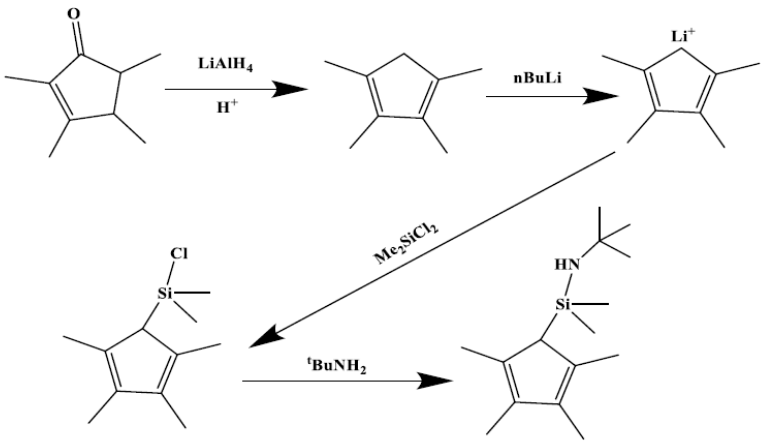

Scheme 1. Synthetic route of $Me_4CpMe_2Si(t\text{-}BuNH)$.

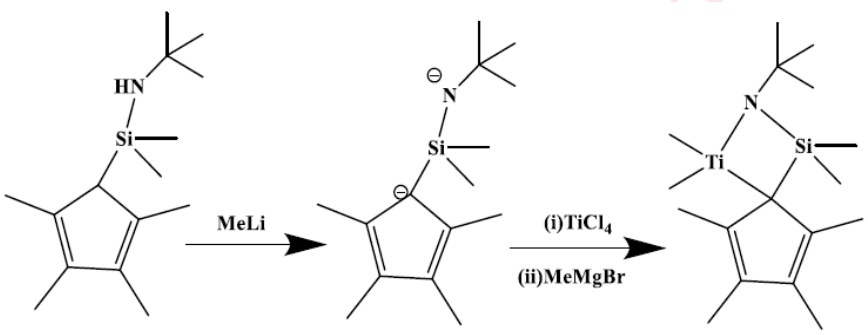

Scheme 2. Synthetic route of $[t\text{-}BuNSiMe_2(Me_4Cp)]TiMe_2$ complex.

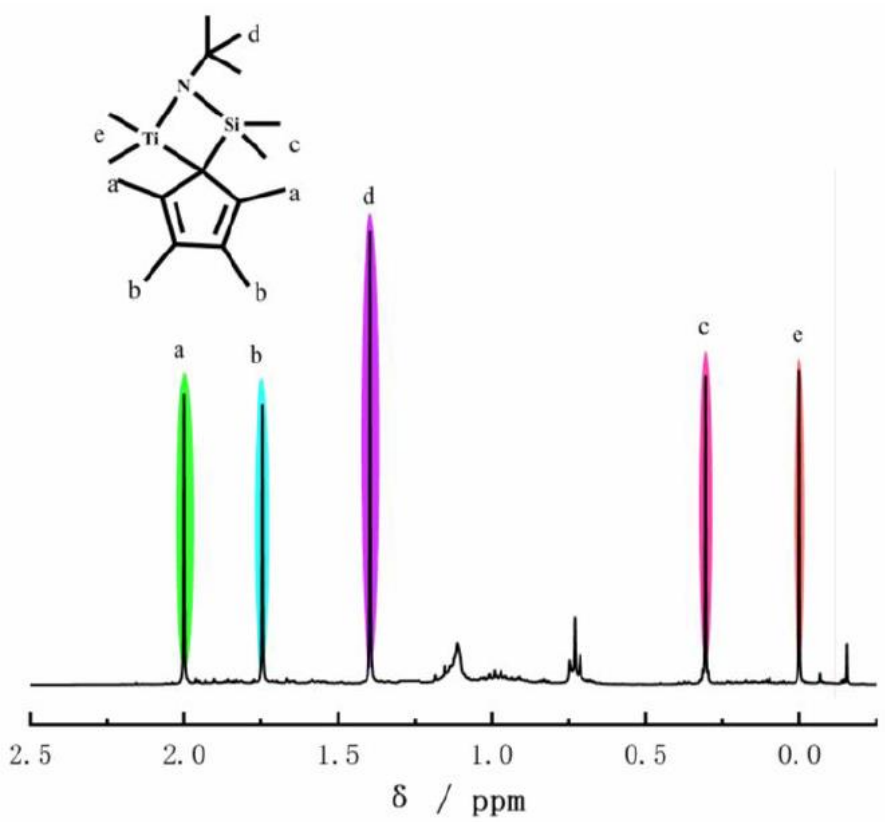

Figure 1. 1H NMR spectrum of [t-BuNSiMe$_2$(Me$_4$Cp)]TiMe$_2$.

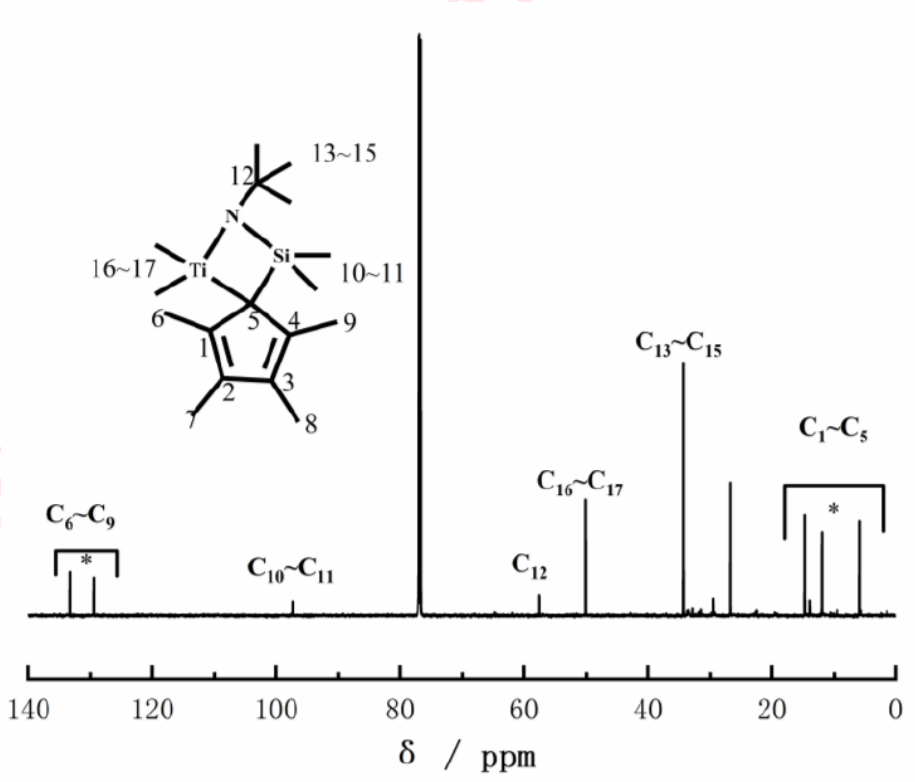

Figure 2. 13C NMR spectrum of [t-BuNSiMe$_2$(Me$_4$Cp)]TiMe$_2$.

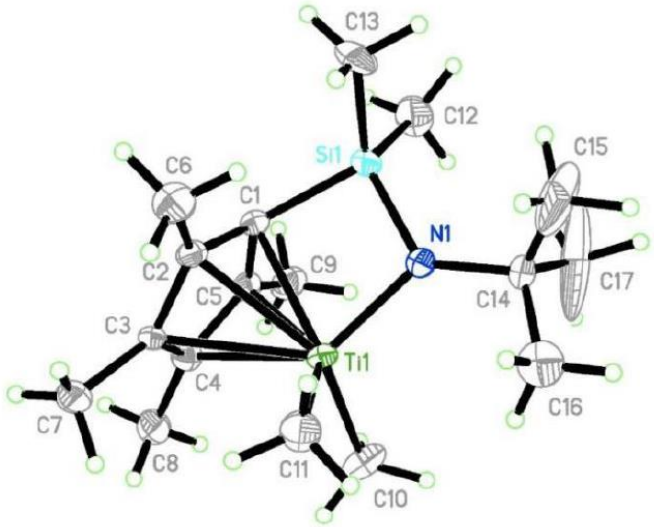

Figure 3. Structure of [t-BuNSiMe$_2$(Me$_4$Cp)]TiMe$_2$ complex.

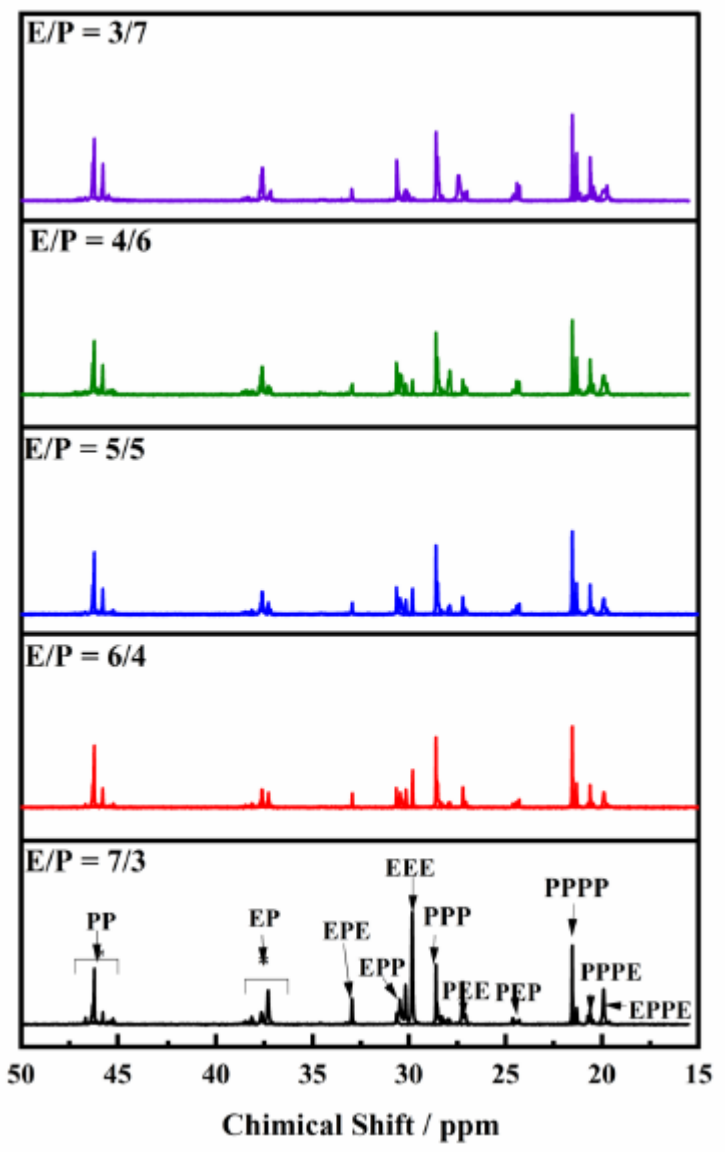

Figure 4. Effect of E/P on sequence distribution of ethylene-propylene random copolymers.

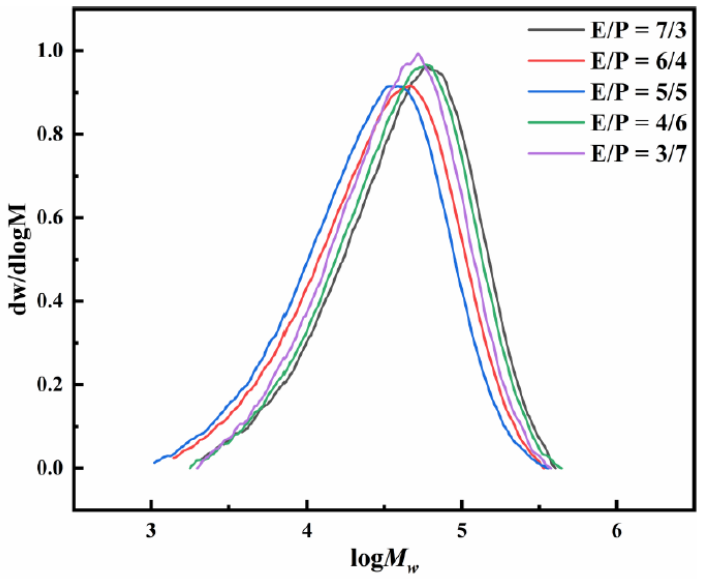

Figure 5. Molecular weight and its distribution curves of ethylene-propylene random copolymers with different E/P.

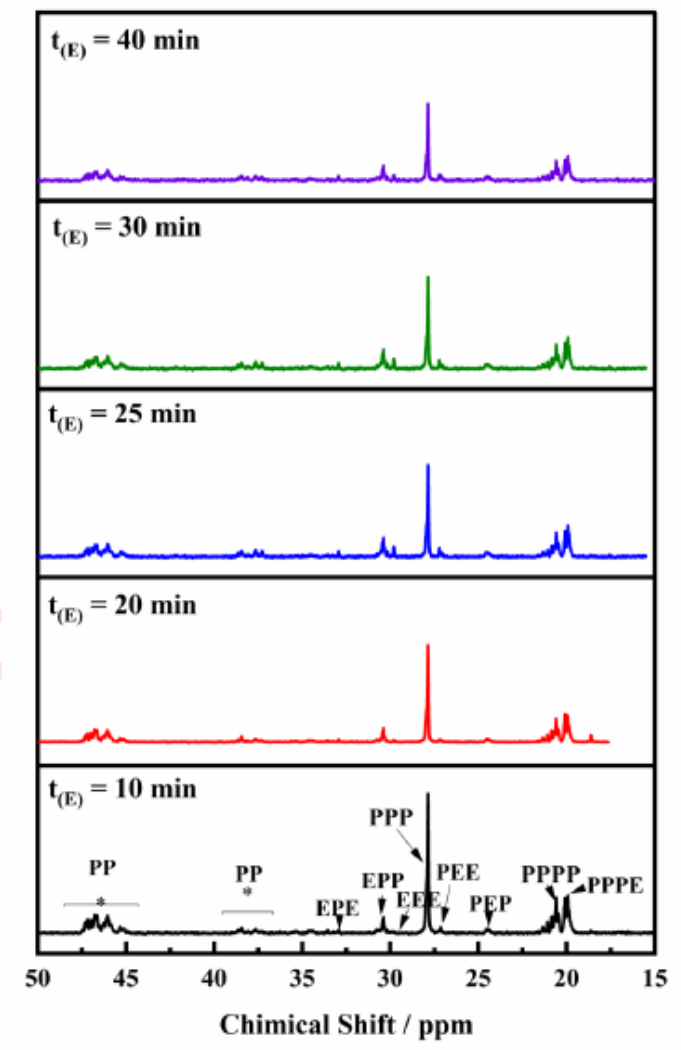

Figure 6. Effect of $t_{(E)}$ on sequence distribution of P-E block copolymers.

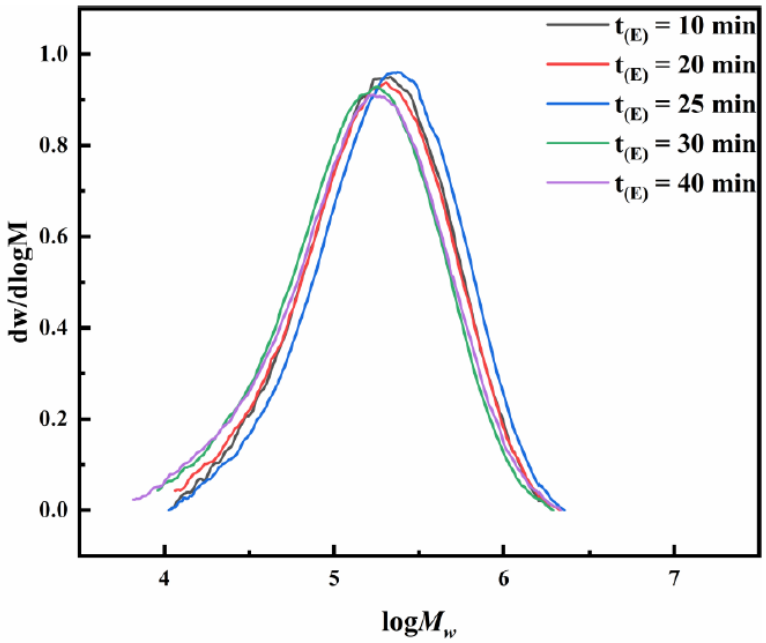

Figure 7. Molecular weight and its distribution curves of propylene-ethylene block copolymers with different $t_{(E)}$.

Table 1. The influence of temperature on ethylene-propylene random copolymerization and copolymers.

Entry	T/℃	Activity/10^3 kg·mol^{-1}h^{-1}	T_g/°C	T_m/°C	T_c/°C
1	40	1.643	-48.9	125.3	110.4
2	50	1.756	-49.3	125.0	108.7
3	60	3.104	-50.1	124.0	78.3
4	70	3.282	-50.1	124.3	-

Polymerization conditions: E/P = 7/3 (partial pressure ratio), polymerization pressure 0.55 MPa, catalyst concentration [Ti] = 9.2×10^{-5} mol/L, Al/Ti = 600, cyclohexane 50 mL, 30 minutes.

Table 2. The influence of E/P on ethylene-propylene random copolymerization and copolymers.

Entry	E/P	Activity/ ×10^3kg·mol^{-1}h^{-1}	T_g/ °C	T_m/ °C	T_c/ °C	$\bar{M}_w$ / 10^4 g/mol	$\bar{M}_n$ / 10^4 g/mol	PDI	E/ mol%	P/ mol%
4	7/3	3.29	50.1	124.3	-	4.98	1.75	2.84	62	38
5	6/4	3.87	49.0	123.4	76.7	5.37	2.04	2.62	59	41
6	5/5	2.38	46.7	121.5	70.7	4.94	1.74	2.83	45	55
7	4/6	4.69	35.1	-	72.5	5.10	2.02	2.53	36	64
8	3/7	5.15	25.0	-	-	5.64	2.33	2.42	32	68

Polymerization conditions: 70°C, polymerization pressure = 0.55 MPa, catalyst concentration [Ti] = 9.2×10^{-5} mol/L, Al/Ti = 600, cyclohexane 50 mL, 30 min.

Calculation method for ethylene and propylene content in ethylene propylene copolymers: P = PPP + PPE + EPE; E = EEE + EEP + PEP.(As shown in Table 2).

Table 3. Composition and sequence distributions of ethylene-propylene random copolymers with different E/P.

	E/P = 7/3	E/P = 6/4	E/P = 5/5	E/P = 4/6	E/P = 3/7
PP	0.10	0.11	0.15	0.16	0.46
EP	0.46	0.50	0.49	0.56	0.33
EE	0.44	0.39	0.36	0.28	0.21
PPP	0.08	0.10	0.17	0.30	0.49
PPE	0.16	0.19	0.28	0.28	0.15
EPE	0.14	0.12	0.10	0.06	0.04
PEP	0.06	0.06	0.04	0.13	0.09
EEP	0.39	0.38	0.26	0.18	0.15
EEE	0.17	0.15	0.15	0.05	0.08
E	0.62	0.59	0.45	0.36	0.32
P	0.38	0.41	0.55	0.64	0.68
RI	0.75	0.75	0.68	0.65	0.43
$r_E \cdot r_P$	0.83	0.69	0.90	0.57	3.55

Table 4. The influence of temperature on P-E block copolymerization and copolymers.

Entry	T/℃	Activity/10^3 kg·mol^{-1}h^{-1}	T_g/℃
9	30	3.47	-4.4
10	40	5.54	-6.9
11	50	8.15	-9.5
12	60	7.81	12.5
13	70	6.25	19.4

Polymerization conditions: polymerization pressure = 0.55 MPa, catalyst concentration [Ti] = 9.2×10^{-5} mol/L, Al/Ti = 600, cyclohexane 50 mL, 20 min.

Table 5. The influence of $t_{(E)}$ ratio on P-E block copolymerization and copolymers.

Entry	$t_{(E)}$/min	Activity/ 10^3kg·mol^{-1}h^{-1}	T_g/℃	$\bar{M}_w$ / 10^4g/mol	$\bar{M}_n$ / 10^4g/mol	PDI	E/mol%	P/mol%
11	10	8.15	-6.9	28.79	12.23	2.35	9	91
14	20	6.06	-9.0	27.87	10.99	2.54	10	90
15	25	5.42	-9.9	25.89	10.86	2.38	12	88
16	30	4.85	-14.6	25.13	9.30	2.70	19	81
17	40	3.92	-15.6	21.37	7.28	2.94	23	77

Polymerization conditions: 50 °C, polymerization pressure = 0.55 MPa, catalyst concentration [Ti] = 9.2×10^{-5} mol/L, Al/Ti = 600, cyclohexane 50 mL.

Calculation method for ethylene and propylene content in ethylene propylene copolymers: P = PPP + PPE + EPE; E = EEE + EEP + PEP.(As shown in Table 6).

Table 6. Composition and sequence distribution of P-E block copolymers with different $t_{(E)}$.

	10min	20min	25min	30min	40min
PP	0.901	0.897	0.837	0.733	0.596
EP	0.095	0.093	0.145	0.176	0.272
EE	0.004	0.010	0.018	0.091	0.132
PPP	0.899	0.784	0.733	0.603	0.482
PPE	0.006	0.116	0.139	0.176	0.256
EPE	0.007	0.005	0.010	0.035	0.028
PEP	0.063	0.055	0.069	0.067	0.097
EEP	0.025	0.039	0.043	0.096	0.111
EEE	-	0.001	0.006	0.023	0.026
E	0.09	0.10	0.12	0.19	0.23
P	0.91	0.90	0.88	0.81	0.77
RI	0.101	0.215	0.261	0.374	0.492
$r_E \cdot r_P$	1.60	4.15	2.87	8.61	4.25